

RESTRICTED DIFFUSION IN BIOPHYSICAL SYSTEMS

EXPERIMENT

ROBERT L. COOPER, DAVID B. CHANG, ALLAN C. YOUNG, CARROLL J. MARTIN, and BETSY ANCKER-JOHNSON

From The Boeing Company, Seattle 98124, the Institute of Respiratory Physiology, Virginia Mason Research Center and Firland Hospital, Seattle 98101, and the University of Washington, Seattle, Washington 98195

ABSTRACT The pulsed-gradient spin echo nuclear magnetic resonance (PGSENMR) technique was used to measure restricted diffusion of water in three types of animal tissue: human blood plasma and red cells; rat and rabbit heart; rat and rabbit liver. Characteristic lengths (L) for restriction of diffusion are estimated from dependence on the measuring time. Limitations on the range of observable restrictive lengths (1.5–15 μm) are discussed.

The decrease in diffusivity due to 1 μm alumina powder (volume fraction = 0.18) in glycerin/water mixtures agrees with the Wang theory assuming spherical particles and no hydration. The characteristic length ($L \simeq 4 \mu\text{m}$) is larger than the particle size (1 μm) or separation (1.8 μm). Comparison of the diffusivities in tissues at short diffusion times with the Wang theory indicates some bound or trapped water.

For packed red blood cells, a restriction ($L \simeq 2.3 \mu\text{m}$) was attributed to the red cell membrane. A permeability $p \simeq 0.014 \text{ cm/s}$ may be estimated from the decrease in diffusivity. Average values of diffusivity ratio in heart were: 0.36 ± 0.02 for rat; and 0.26 ± 0.03 for rabbit; and in liver: 0.25 ± 0.01 for rat; 0.25 ± 0.04 for 10-day old rabbit; and 0.195 ± 0.03 for 2-yr old rabbit. A restriction ($L \simeq 2.7 \mu\text{m}$) in rat liver probably results from the mitochondria.

INTRODUCTION

Water diffusion in animal tissues and related model systems has been studied (1) by means of the pulsed-gradient spin echo nuclear magnetic resonance (PGSENMR) technique for measuring restricted diffusion. We present here an attempt to describe the results of these measurements in terms of simple theoretical models available in the literature. A general theory of PGSENMR measurements will be published elsewhere.

Recent interest in the state of water in tissues has raised questions regarding the properties of water itself (2) and the interactions of water with the intracellular environment. The diffusivity of water may be modified by interaction with dissolved

macromolecules and colloidal particles (3) or diffusion may be restricted by the inhomogeneous structure of the tissue (4, 5). The PGSENMR technique (6-8) is ideally suited to study the diffusion of water in the presence of restrictions comparable with the cellular structures of many animal tissues. Nuclear magnetic resonance (NMR) techniques using steady gradients (4, 9) have been used (10-13) to look for restrictions with characteristic lengths between 8 and 15 μm . The PGSENMR technique can be used in the range 1.5-15 μm .

The usual methods of measuring diffusion first establish a gradient in the concentration of a labeled material in the sample under test and then determine the rate at which the labeled material is transported along the gradient. These methods have certain disadvantages. There is danger of disrupting the system either while introducing the labeled material or while osmotic forces are active. Properly weighted average values are obtained only after transients have disappeared.

NMR methods of measuring diffusion avoid these effects: no foreign material is introduced, the system remains in osmotic equilibrium, and average diffusivities are weighted by the equilibrium particle distribution. The presence of a magnetic field gradient labels one species of atomic nuclei in the system under study as a function of their position along the gradient without otherwise disturbing the system. Diffusivities along this gradient are averaged over the time during which the measurement is made within a restricted range of times. The upper limit for the time is set by the relaxation time (T_2) of the precessing component of magnetization of the nuclei. The lower limit is set by the magnitude of the gradient which can be applied.

The PGSENMR technique has certain advantages over the steady gradient NMR technique. First, the time (Δ) between gradient pulses provides a definite time rather than a wide distribution of times during which the diffusion is measured. Second, the value of Δ may be varied independently of the time (τ) separating the radio-frequency (RF) pulses, thus avoiding uncertainty regarding the effects of changing the time τ . Third, the magnitude of the gradient used in the pulses can be made much larger than in the steady gradient method because the pulsed gradient can be reduced to a very small value at the time the RF pulses are applied. This permits the use of shorter diffusion times which make it possible to observe restricted water diffusion effects having characteristic lengths as small as 1.5 μm .

Several experiments are considered in which the PGSENMR technique has been used to observe restricted diffusion in animal tissues and related model inhomogeneous systems. Under Materials and Methods, the apparatus, procedures for taking and evaluating data, sources of materials, and methods of preparing samples are described. Under Results, PGSENMR measurements are presented for certain non-biological samples and for three types of animal tissues: blood fractions (human); heart (rat and rabbit); and liver (rat and rabbit). Under Theory and Discussion, the significance of the results is discussed in terms of the effects on diffusion of water expected from the dispersion of small particles and macromolecules, restriction by

the cell plasma membrane, and restriction by organelle membranes or other intracellular structures. The limits on the range of characteristic restrictive dimensions observable by the PGSENMR technique are discussed.

MATERIALS AND METHODS

General Procedures

The PGSENMR technique for measuring restricted diffusion has been applied to two types of materials. Nonbiological samples were prepared from purified materials to form systems with well defined properties, such as diffusion coefficient and particle size to provide simple controlled systems simulating conditions expected in animal tissues. Biological samples were prepared from animal tissues available in research programs under way at the Institute for Respiratory Physiology. Materials and tissues used for these diffusion measurements were placed in 12 mm diameter \times 75 mm round bottom culture tubes, sealed with rubber stoppers, and positioned in the RF coil of the PGSENMR spectrometer so as to provide the maximum echo with gradient pulses off. All measurements were made at room temperature (about 25°C).

Spectrometer Specifications

A block diagram of the Boeing PGSENMR spectrometer is shown in Fig. 1. It is a conventional spin echo spectrometer, similar to that described by Lowe and Tarr (14) except that a 15-turn, series-tuned, radio-frequency coil is used. Provisions for generating the magnetic field gradient pulses are similar to those described by Tanner (15) except that a peak current regulator has been added. A residual gradient (about 0.1 G/cm) is used to stabilize the spin echo shape. The static magnetic field (H_0) is provided by a 12 in Varian magnet (V-4012-3B; Varian Associates, Palo Alto, Calif.) with 3 in gap and current regulated power supply (V-2100B). The field was continually reset to maintain protons in resonance (± 400 Hz). The receiver is a modified Matec (main-frame 6000 plug-in 960; Matec, Inc., Warwick, R.I.). The apparatus is controlled by an F & H Instruments (PPG-45) pulse program generator (F & H Instruments, Gaithersburg, Md.). The significant parameters and usual range of values are in Table I.

Spectrometer Operation

The pulse program was set and allowed to sweep repeatedly with the gradient pulses alternately on and off as shown in Fig. 2. The echoes were monitored until satisfactory settings were obtained for all parameters. Then 5–20 oscilloscope traces extending for 10 ms centered on the spin echo were photographed for each set of parameters. In order to establish a zero the second gradient pulse was omitted for 5–20 sweeps on each photograph. A sequence of values of Δ , g , and δ was set to provide 3–10 values of spin echo attenuations between 10 and 95% of the echo amplitude without gradient pulses. Each photograph could accommodate from three to six sets of parameters. A typical data run is shown in Fig. 3.

The repetition period T_0 was varied only to estimate the relaxation time T_1 (energy changing). It was found that choosing $T_0 > 3 T_1$ was sufficient to suppress interfering effects from previous sweeps. The interval τ between RF pulses was usually varied only to roughly estimate the relaxation time T_2 (energy conserving) or to explore for beats in spin echo amplitude which can result from interactions between protons located in the same molecule. Prominent beats were found in pure liquids such as isopropanol and aniline but not in other samples.

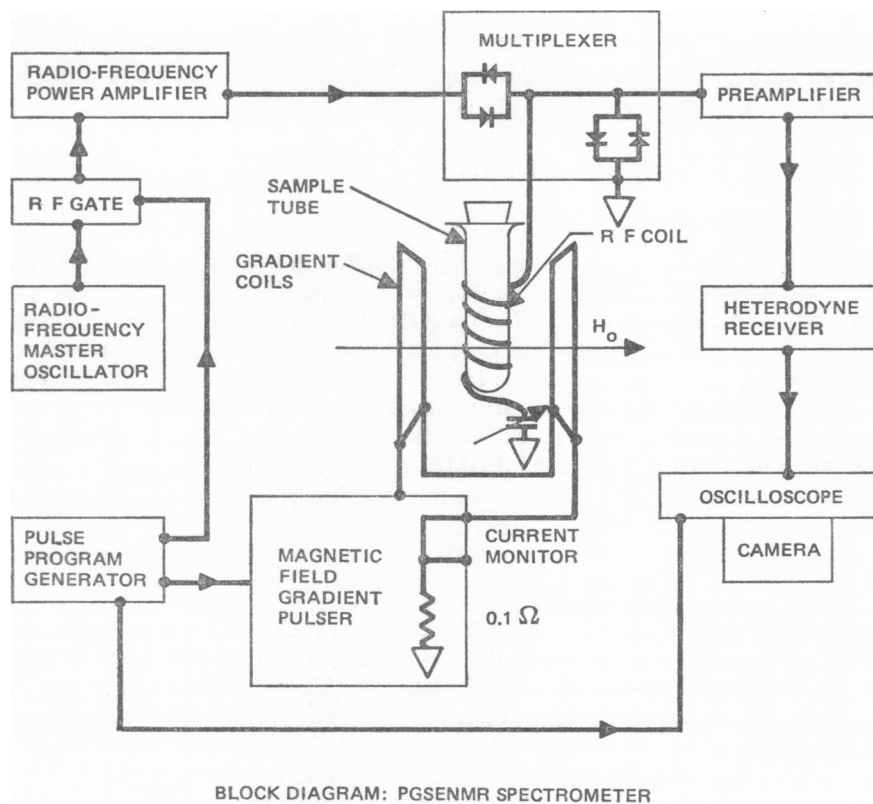


FIGURE 1 Block diagram of PGSENMR spectrometer.

TABLE I
PGSENMR SPECTROMETER PARAMETERS

Symbol	Definition	Values	Units
T_o	Sweep repetition period	1-8	s
τ	Interval between RF pulses	10-100	ms
T_{90}	Width of first RF pulse	7	μ s
T_{180}	Width of second RF pulse	12-13	μ s
f_o	Oscillator frequency	$38,009.7 \pm 0.1$	kHz
A_{max}	Spin echo from 1 ml H_2O into 50 Ω load	100	μ V (rms)
A_{min}	Preamp input noise (200 kHz band)	0.5	μ V (rms)
Δ	Interval between gradient pulses	2-100	ms
g	Strength of gradient pulse	50-200	G/cm
τ_g	Gradient rise and fall time constant	100	μ s
δ	Nominal width of gradient pulse	0.15-1.50	ms
$\delta_1 - \delta_2$	Adjustable pulse width difference	± 50	μ s
T_g	Nominal separation of gradient and RF pulses	0.5-50	ms

rms, root mean square.

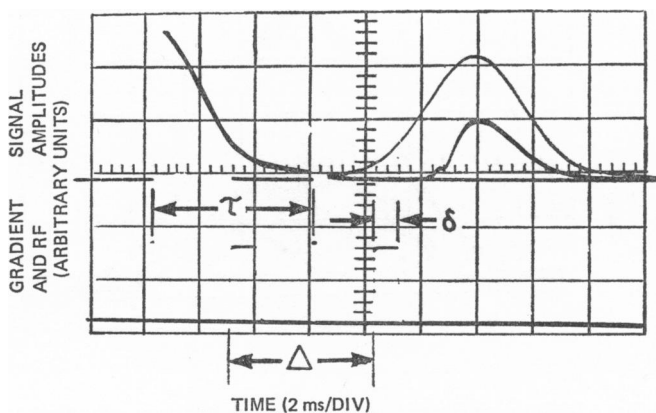


FIGURE 2 Pulse program and resulting signals. The 2 RF (trigger) pulses are separated by the interval τ . The gradient (current) pulses are separated by the interval Δ and have widths δ . After the first RF pulse a free precession signal appears. In the absence of the gradient pulses, this persists until interrupted by the second RF pulse. Following this the full spin echo appears (upper trace) with peak at the time 2τ . When the first gradient pulse occurs, the free precession is immediately quenched. In the absence of a second gradient pulse the signal remains zero. If the second gradient pulse occurs and compensates for the first pulse, an attenuated echo recovers with peak close to the time 2τ . The delay in rise of the attenuated echo is the result of gradients caused by eddy currents following the second gradient pulse.

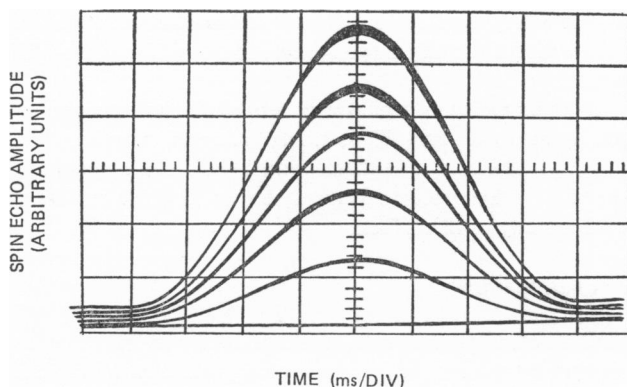


FIGURE 3 Typical data sequence. Sample: 47% Gly/H₂O mixture. Settings: $\tau = 40$ ms; $\Delta = 30$ ms; $g = 130$ G/cm; upper trace with gradient pulses off; other traces with $\delta = 0.30, 0.42, 0.60, \text{ and } 0.84$ ms; lower (zero) trace with only first gradient pulse on.

Most of the data were taken with T_0 and τ held constant. In order to maintain good signal to noise ratios for small samples having short T_2 , values of $\Delta < 15$ ms were taken with $\tau = 10$ ms. Longer values of Δ then required a change to $\tau = 20$ ms (or longer) with consequent loss in signal to noise ratio. The effect of changing τ on the diffusion measurements has been checked several times, but no dependence of D/D_w on τ outside of experimental uncertainty has been observed.

The vernier controls on the gradient pulse widths were set to maximize the amplitude of

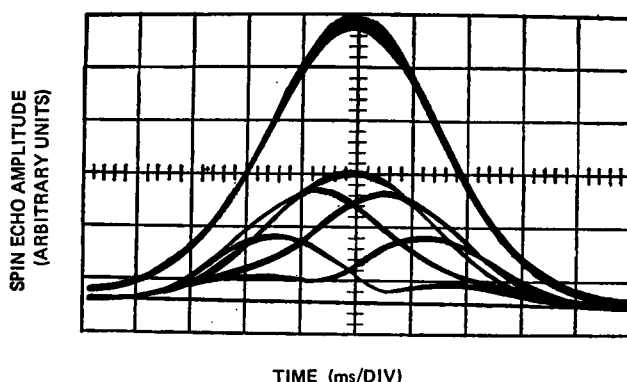


FIGURE 4 Effect of failure of second gradient pulse to compensate for first pulse. Upper trace with gradient pulses off. Zero trace with only first gradient pulse on. Remaining traces with $g = 200$ G/cm and $\delta = 1,000 \mu\text{s}$ (nominal). The five traces result from changing the first gradient pulse width (δ_1) in steps of $0.5 \mu\text{s}$.

the spin echo. Usually this also located the peak of the echo at the expected time 2τ after the first RF pulse. This adjustment was necessary to assure that $\delta_1 - \delta_2$ would compensate for small changes in the effective strength g for closely spaced gradient pulses. In Fig. 4 the effect of lack of compensation is shown on a photograph of five well-separated echoes that result from changing the first gradient pulse width in steps of 0.05% .

It should be noted that errors in compensation by the second gradient pulse can result only in *decreased* values of echo amplitude. This will lead to *increased* effective values of diffusivity. Consequently, for data with unusually large scatter, the larger values of diffusivity are most likely to be in error.

Difficulties were encountered with rapid dependence of echo attenuation on T_0 when the second RF pulse was applied too soon ($T_0 < 1.4$ ms) after the nominal end of the first gradient pulse. This is not predicted by simple theories of the effect of magnetic field gradients but may result from overlap of these pulses. Data taken under these conditions have been excluded, pending further study of this effect.

Evaluation of Diffusivities

For an ideal PGSENMR measurement with constant diffusivity, rectangular gradient pulses, and exact compensation by the second gradient pulse, one obtains the Tanner-Stejskal (5) relation

$$\ln (A_0/A_i) = D\gamma^2(g\delta)_i^2(\Delta - [\delta/3]), \quad (1)$$

where A_0 is the spin echo amplitude without gradient pulses, A_i the amplitude for the i th setting of $g\delta$, and γ is the nuclear gyromagnetic ratio. For the proton the value $\gamma/2\pi = 4,258$ Hz/G was used. Eq. 1 holds for all values $0 \leq \delta \leq \Delta$ and reduces to the Carr-Purcell (9) expression

$$\ln (A_0/A_i) = D\gamma^2 g_i^2 (2/3)\tau^3, \quad (2)$$

in the steady gradient case for which $\delta = \Delta = \tau$.

The magnetic field gradient (g) for the pulses was not measured directly. Instead a value $D_w = 2.5 \times 10^{-5} \text{ cm}^2/\text{s}$ was assumed for the diffusivity of deionized water and effective values of g were calculated from Eq. 1 for set values of Δ , δ , and gradient current I_g . These were then assumed to hold for other samples at the same values of Δ , δ , and I_g , and Eq. 1 was used to calculate effective values of diffusion coefficient (D). In order to avoid any bias from the assumed value of D_w , we report values of D/D_w .

Evaluation of Restrictive Lengths

If there is no restriction of diffusion, a plot of D/D_w as a function of $\Delta - \delta/3$ should be independent of Δ . In the presence of restrictive microbarriers, the observed diffusion coefficient is expected (see Discussion) to change from a short-time value D_s for intervals $\Delta \ll \Delta_R$ to a restricted value D_R for $\Delta \gg \Delta_R$ (see Fig. 5). The characteristic interval Δ_R is defined empirically by the value of the measuring interval $\Delta_R - \delta/3$ at which the decreasing diffusion coefficient reaches the value $D = (D_s + D_R)/2$. In terms of this interval we may define a characteristic restrictive length $L = (2D_s[\Delta_R - \delta/3])^{1/2}$.

The ratio D/D_w could also depend on the parameters g and δ . However, none of the experiments reported here show statistically significant dependence when treated as a function of more than one of the variables Δ , g , and δ .

Model Systems

The viscous solutions used in these studies were prepared from Baker USP glycerin (2140; J. T. Baker Chemical Co., Phillipsburg, N.J.) and distilled water. The powder was Linde semiconductor grade (1.0 C) micron alumina. It was added to the sample tube first and tamped with a Teflon rod. Then the glycerin/water solution was added. There was usually some settling of the powder during the first few minutes leaving a little free solution in a meniscus, estimated to be less than 1% of the solution. The gelatine sample was prepared from unflavored Knox gelatine and distilled water.

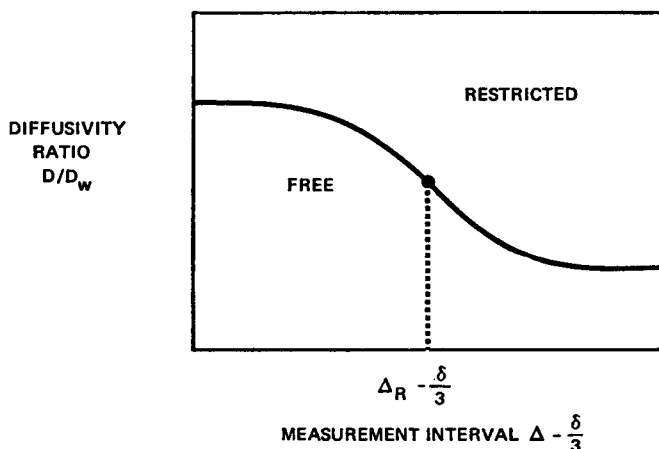


FIGURE 5 Dependence of diffusivity ratio (D/D_w) on the effective duration of the measurement ($\Delta - \delta/3$). For small Δ water is free to diffuse. For large Δ water diffusion is restricted. Dotted line indicates interval $\Delta_R - \delta/3$ used to determine characteristic length $L = (2D_s[\Delta_R - \delta/3])^{1/2}$.

Human Blood Fractions

A sample of blood was obtained from a patient with pulmonary tuberculosis, centrifuged, and separated into three fractions: packed red blood cells, blood plasma, and white blood cells. The plasma was free of hemolysis. The volume of white blood cells was too small for study.

Animal Tissues

Samples were obtained from six Sprague-Dawley rats and two New Zealand white rabbits. Animals were anesthetized with nembutal (75 mg/kg), the abdomen opened and the left renal artery severed. Following exsanguination the contents of the chest cavity were removed for study. The heart and remains were placed on ice and transported to the PGSENMR laboratory. All tissue studies were treated in the same time sequence.

Heart

Samples were prepared from the heart first. The lower portion (about 0.7 g) of the ventricles was excised and cleaned with a cotton swab, and PGSENMR measurements were made for a period of 4–8 h. Data taken within 1 h of death were reproducible and consistent with data from other animals up to 10 h after sacrifice.

Liver

The remains were stored in a refrigerator between 0 and 5°C until studies could be continued on the following day. The liver was removed from the animal and a sample (about 0.8 g) prepared from two or more cylindrical sections excised from a main lobe, freed from excess fluid and damaged cells by contact with the glazed surface of the dissecting plate, and studied for 4–8 h.

RESULTS

Measurements of the diffusivity of water have been made using the PGSENMR technique for several model systems and animal tissues. The principal results for the ratio of the diffusivity (D) to the diffusivity of pure water (D_w) and the characteristic restrictive dimensions (L) are shown in Table II.

Nonbiological Samples

Mixtures containing 0.0, 26.4, and 47.1 % by weight glycerin/water were examined with and without 1 μm diameter alumina powder. Results for the six systems are shown in Fig. 6. When compared with values of viscosity (η) found by interpolation from tables (16), the measured diffusivities (D) satisfied the Sutherland-Einstein relation (17): $E = D_{\text{mix}}\eta_{\text{mix}}/D_w\eta_w$ fairly well, $E \simeq 1.06$ and 1.23 for 26 and 47 % glycerine/ H_2O , respectively.

The same concentrations of solution were in the tubes containing 1 μm diameter alumina powder. Assuming a density of 4 g/ml for alumina, the volume fraction of alumina was calculated to be 0.18 for all three samples. The observed restrictive dimension $\simeq 4 \mu\text{m}$ characteristic of these systems is much larger than either the par-

TABLE II
PGSENMR MEASUREMENTS OF WATER DIFFUSIVITY RATIO AND RESTRICTIVE
DIMENSIONS IN MODEL SYSTEMS AND ANIMAL TISSUES

Type of sample	Diffusivity ratio D/D_0			Restrictive dimensions μm
	Small Δ	Mean \pm SD	Large Δ	
Dispersed mixtures				
100% H ₂ O	—	1.00	—	—
26% Gly/H ₂ O	—	0.50 \pm 0.02	—	—
47% Gly/H ₂ O	—	0.25 \pm 0.02	—	—
15% gelatine/H ₂ O	—	0.7 \pm 0.1	—	—
1 μm alumina mixes				
Pure H ₂ O	0.95	—	0.75	$L \simeq 5$
26% Gly/H ₂ O	0.45	—	0.40	$L \simeq 4$
47% Gly/H ₂ O	0.24	—	0.18	$L \simeq 4$
Blood fractions				
Plasma	—	0.86 \pm 0.02	—	—
Red cells	0.22	—	0.08	$L = 2.3 \pm 0.4$
Heart tissue				
Rat	(0.37)	0.36 \pm 0.02	(0.34)	($L \simeq 10$)
Rabbit (2 yr)	—	0.26 \pm 0.03	—	—
Liver tissue				
Rat	0.30	—	0.25	$L \simeq 2.7$
Rabbit (10 day)	—	0.25 \pm 0.04	—	—
Rabbit (2 yr)	—	0.195 \pm 0.03	—	—

ticle size (1.0 μm) or the average distance between centers of alumina particles (1.8 μm) (see Discussion).

The gelatine sample contained 15% by weight (as packaged) Knox gelatine. The residual moisture content was not determined. The data were not sufficient to determine if a restricted diffusion effect might be present.

Human Blood Fractions

Results of measurements on separated blood fractions are shown in Fig. 7. For the blood plasma, data were insufficient to determine the presence of restrictive diffusion and the straight line indicates the mean value of all the measurements. No determination of protein content was made for this sample.

For the packed red cells the decrease in diffusivity ratio from 0.22 for $\Delta \simeq 2.2$ ms to 0.08 for $\Delta \simeq 16$ ms corresponds to restrictive dimensions between 1.5 and 4.0 μm with the most probable value at 2.3 μm . The slow transition is expected for a nonspherical cell (diameter 8 μm and thickness 2 μm).

Heart Tissue

Samples from rats varying in age from 6 to 11 mo showed no significant difference in diffusivity ratio, and the results for six rat hearts were combined and shown in

Fig. 8. As discussed under spectrometer operation, errors tend to be biased toward higher values of D/D_w . Consequently the decrease in diffusivity ratio as $\Delta - \delta/3$ goes from 2.2 to 10 ms cannot be regarded as significant. A small but definite ($9 \pm 6\%$) decrease in D/D_w as Δ goes from 20 to 60 ms indicates the presence of a slight restriction with a characteristic dimension near $10 \mu\text{m}$. If we neglect these small effects we obtain the average value indicated by the straight line.

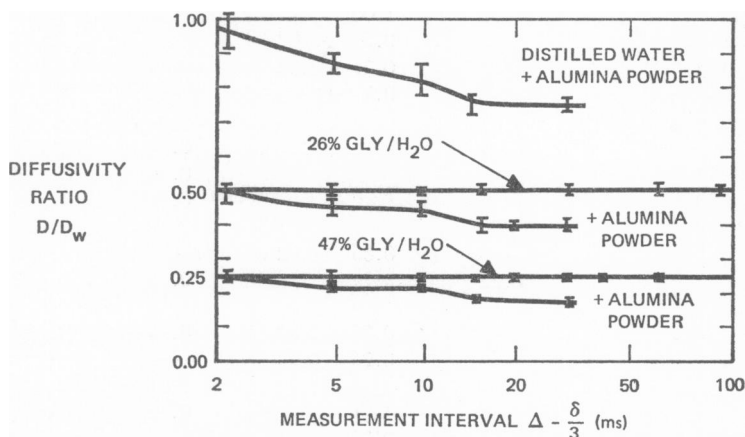


FIGURE 6 PGSENMR results for glycerin/water mixtures with and without 18 vol % of $1 \mu\text{m}$ diameter alumina powder. Diffusivity ratio (D/D_w) is defined as 1.00 for distilled water. Mean value ± 1 SD shown for 4–10 measurements varying $g\delta$ at fixed Δ . The decreases in D/D_w with increase in Δ for mixtures including alumina powder indicate restrictions with characteristic lengths near $4 \mu\text{m}$.

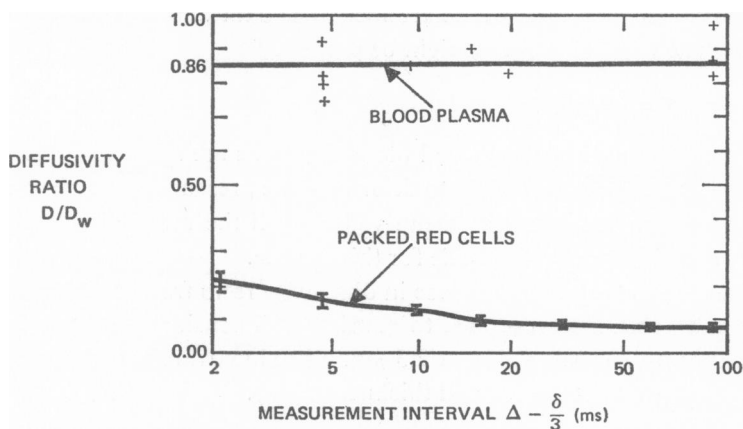


FIGURE 7 Results of PGSENMR measurements for human blood fractions. For the plasma all measured values of D/D_w are shown. The solid line at $D/D_w = 0.86$ indicates mean value. For the packed red cells mean values ± 1 SD shown for 3–10 measurements varying $g\delta$ at fixed Δ . Decrease in D/D_w with increasing Δ indicates restriction near $2.3 \mu\text{m}$.

No evidence was found for restricted diffusion in the rabbit heart. A decrease as small as that found in rat would have been obscured by variability in D/D_w ($\pm 12\%$).

Liver Tissue

No dependence on age was found, and the data for the six rat livers were combined and shown in Fig. 9. A decrease in D/D_w from 0.30 to 0.25 for $\Delta - \delta/3$ near 5 ms corresponds to a restrictive dimension near 2.7 μm . The mean value and standard error of the asymptotic value of $D/D_w = 0.250 \pm 0.006$ for rat liver.

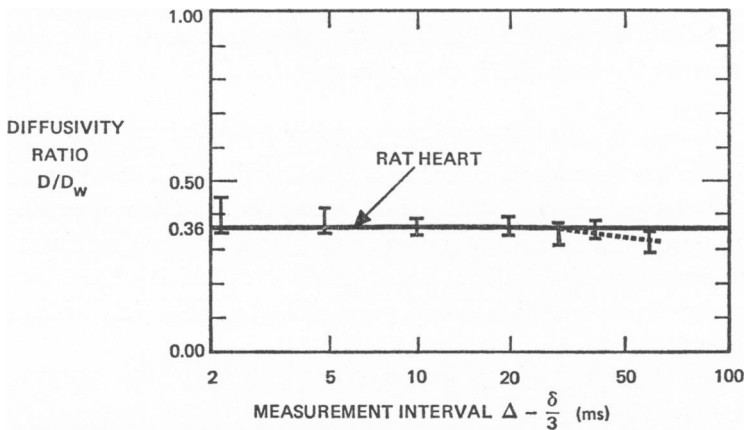


FIGURE 8 Results of PGSENMR measurements for six rat hearts. Mean value ± 1 SD shown for about 25 measurements varying $g\delta$ at fixed Δ . Decrease in D/D_w for $\Delta > 20$ ms indicates restriction near 10 μm (or larger). The solid line indicates mean value for all the data.

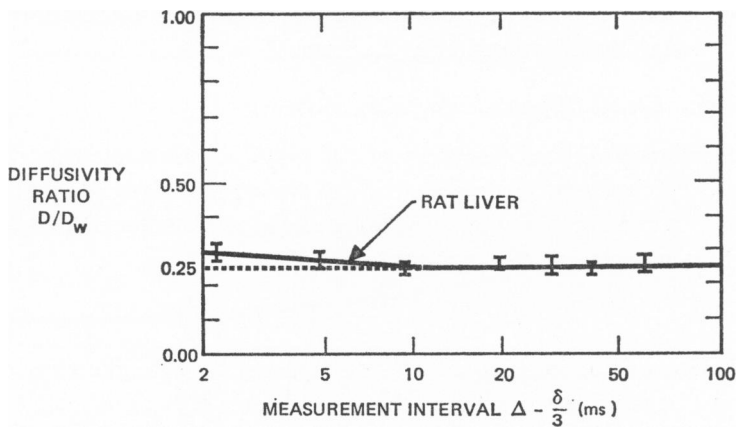


FIGURE 9 Results of PGSENMR measurements for six rat livers. Mean value \pm SD shown for about 25 measurements varying $g\delta$ at fixed Δ . The solid line indicates the asymptotic value of diffusivity ratio $D/D_w = 0.250 \pm 0.006$ for $\Delta > 10$ ms. The decrease in diffusivity ratio for increasing Δ indicates a restriction near 2.7 μm .

For the rabbit livers a similar decrease in D/D_w is possible but obscured by insufficient data. Average values of diffusivity ratio show a 24 % dependence upon age of the rabbits.

THEORY AND DISCUSSION

Restricted Diffusion Effects

The reduced diffusivity of intracellular water can result in part from the presence of dispersed macromolecules and particles of comparable size (3). It can also result in part from the presence of larger components of the cell structure (4, 5). The PGS-ENMR technique is capable of distinguishing between these contributions to restricted diffusion by determining the dependence of diffusivity D on measuring interval Δ .

Several theoretical studies have been made of restricted diffusion in systems involving simple configurations of impenetrable barriers (8). In these systems, for which the diffusing molecules are completely trapped, as Δ increases, the spin echo amplitude approaches an asymptotic value (neglecting relaxation times T_1 and T_2) which is independent of Δ and also independent of diffusivity (5). Such models are not appropriate for water diffusion in most biological materials which are usually quite permeable to water.

No detailed theory of restricted diffusion is available even for simple models appropriate for suspended particles or biological materials. However, several approximate calculations can be made. For restrictions having a characteristic interval Δ_R , the short-time diffusivity D_s for intervals $\Delta \ll \Delta_R$ is large because only a small fraction of the diffusing molecules have encountered a barrier. If the barriers consist of suspended particles or penetrable membranes, the restricted diffusivity D_R for $\Delta \gg \Delta_R$ approaches a small asymptotic value because then all diffusing molecules have equal probability of encountering barriers.

Restriction by Dispersed Materials

If the material is all dispersed in the form of small impenetrable particles, and we neglect the exchange between free and bound water, the Wang (3) theory predicts that for large Δ the diffusivity approaches an asymptotic value D_R . The diffusivity ratio may then be conveniently expressed in the form:

$$D_R/D_w = 1 - \beta(1 + h)f_p, \quad (3)$$

where β is a geometrical factor equal to 1.5 for spheres, f_p is the effective volume fraction occupied by the dry protein (or other solids) after dispersion, and h is an effective hydration factor. The factor h can result from several contributions which would be difficult to distinguish. For example, permanently or temporarily bound or trapped water can increase the effective volume of the molecules, and the delay caused by temporary binding can increase the effective path length for diffusion.

Estimation of Restrictive Dimension

The characteristic restrictive length for a suspension of particles may be estimated by analogy with the kinetic theory of collisions. If we denote by $p(\Delta)$ the probability that a diffusing molecule has not encountered a barrier during the interval Δ , then the average diffusion coefficient is given roughly by

$$D(\Delta) = D_s p(\Delta) + D_R (1 - p(\Delta)).$$

From the definition of Δ_R we have $D(\Delta_R) = \frac{1}{2}(D_s + D_R)$, so that $p(\Delta_R) = \frac{1}{2}$.

In the case of diffusion through a suspension of restricting particles with number density $N = f_v/V_0$, where f_v is the volume fraction and V_0 is the particle volume, and cross-section σ , $p(\Delta)$ may be estimated from the usual mean free path expression for the probability that a molecule escapes collision with a particle after traversing a net distance x : $P(x) = \exp(-xN\sigma)$. Assuming that the diffusion random walk step length is much less than the distance between particles, we set x equal to the root mean square displacement $(2D_s[\Delta - \delta/3])^{1/2}$. Defining the particle size by $d = V_0/\sigma$, we have

$$L = (2D_s[\Delta_R - \delta/3])^{1/2} = -\ln(p(\Delta_R))/N\sigma = d \ln 2/f_v.$$

Applying this result to the samples of micron alumina particles with measured volume fraction $f_v = 0.18$, and setting $d = 1 \mu\text{m}$, we obtain $L = 3.8 \mu\text{m}$ for the predicted value, in good agreement with the experimental estimate of $L \simeq 4 \mu\text{m}$.

Restriction by Cell Membrane

The appropriate model for the cell plasmalemma is a closed permeable membrane. For simplicity we assume this to consist of a set of parallel membranes perpendicular to the applied magnetic field gradient which determines the direction in which the diffusivity is measured. This is the model cited by Crick (18) in his discussion of morphogen diffusion. By considering the resistance to a steady flux, it is seen that for diffusion through a series of membranes which have a permeability p and a separation distance L , the effective diffusion coefficient is given by

$$1/D_R = 1/D_s + 1/pL, \quad (4)$$

where D_s is the diffusion coefficient in the region between the barriers. When D_R , D_s , and L can be estimated from the PGSENMR measurements, a value of the membrane permeability may be calculated.

Restriction by Intracellular Structures

If the restriction results from membranes surrounding small organelles, such as mitochondria, or composing open extended organelles, such as endoplasmic reticu-

lum, the restrictive dimension could be related to both the size of the organelles and the average distance between organelles as well as the membrane permeability. In order to avoid this complexity, one may apply the Wang theory but replace D_w by D_s , the value found for $\Delta = \Delta_s \ll \Delta_R$. This will give an equivalent value

$$f_R = [(1 + h)f_p]_{\text{eff}}, \quad (5)$$

for the effective volume fraction of the cell that is contributing to the restriction with dimension L for times $\Delta \simeq \Delta_R$.

Other Effects

For inhomogeneous systems as complicated as biological tissues, questions arise as to which cellular structures provide restrictions. Also, the possibility that other effects besides restriction of diffusion may contribute to the observed dependence of diffusion on the measuring interval must be considered. For example, Tanner and Stejskal (5) discussed the case of a system of two nonexchanging components with different diffusivities. Similar systems with finite exchange rates or different relaxation times could also be considered. Introducing these complications would require additional parameters in the theory. Since the data obtained in the PGSENMR experiments considered here are not capable of providing a base for evaluating these additional parameters, we confine the discussion to the question: Can the PGSENMR results be described in terms of appropriate simple models of restricted diffusion?

Examples of Restricted Diffusion

Three cases applying Eq. 3, 4, or 5 to appropriate portions of the PGSENMR results are illustrated below: (a) Eq. 3 is used to test the postulate that for the smallest values of Δ used in the measurements the material appears dispersed; (b) Eq. 4 is used to estimate a membrane permeability for a case where the characteristic restrictive dimension L may be identified with the cell size; and (c) Eq. 5 is used to estimate an effective volume fraction for cases where the characteristic restrictive dimension is too small to be identified with the cell size.

(a) Since the water contents of the tissues used for the PGSENMR measurements were not determined, the volume fractions of solids f_p are estimated from tables (19, 20). Predictions of the Wang theory for dispersed spherical particles and three values of hydration factor (h) are compared with values of D/D_w observed at small Δ — $\delta/3 \simeq 2.2$ ms in Table III. In all cases the observed diffusivities require a hydration factor $h \gtrsim 0.5$, which may result from water bound to the protein. The larger values of h required by cellular tissues may result from water trapped by the smaller organelles.

(b) The derivation of Eq. 4 assumed that L was the distance between membranes

TABLE III
COMPARISON OF DIFFUSION OBSERVED AT SMALL DIFFUSION TIME
WITH PREDICTION FOR DISPERSED MATERIAL

Type of tissue studied	Vol % water 100 f_w	Vol % solids 100 f_p	Diffusivity ratio D/D_w			Observed at small Δ
			$h = 0.0$	$h = 0.5$	$h = 1.0$	
Plasma	94	6	0.910	0.865	0.820	0.86
Red cells	72	28	0.580	0.370	0.160	0.22
Heart	77	23	0.655	0.482	0.310	0.37
Liver	71	29	0.565	0.348	0.130	0.30

h , hydration factor.

oriented perpendicular to the direction of diffusion. If we identify the characteristic dimension ($L \simeq 2.3 \mu\text{m}$) for red cells as an effective value of the L of Eq. 4, and the value of diffusivity found at small Δ ($D_s/D_w \simeq 0.22$) as the D_0 of Eq. 4, the asymptotic value ($D_R/D_w \simeq 0.08$) and water diffusivity $D_w = 2.5 \times 10^{-5} \text{ cm}^2/\text{s}$ give a value for the membrane permeability: $p = 0.014 \text{ cm/s}$. This compares with reported values (21, 22) of osmotic permeability (0.0127 cm/s) and tracer (TOH) permeability (0.0053 cm/s). A theory for a more realistic model of packed red blood cells will be required for proper interpretation of the PGSENMR result.

(c) For the model systems, we use the measured values for the diffusivities without alumina powder. For rat heart and liver we must use the values measured for $\Delta - \delta/3 \simeq 2.2 \text{ ms}$. The assumed values and results of calculating the effective volume fraction (f_R) from Eq. 5 are shown in Table IV. The effective volume fractions calculated for the model systems agree fairly well with the measured value 0.18, assuming no hydration. The observed restrictive dimensions (L) are about four times the particle diameter. For rat liver, the effective volume fraction is near that for the model systems. This makes it reasonable to attribute the restriction with characteristic dimension $L = 2.7 \mu\text{m}$ to particles about $0.7 \mu\text{m}$ in diameter, suggesting the numerous mitochondria seen in electron micrographs (23). This identification agrees well with the morphometric measurements of Weibel et al. (24) who found the liver (rat) mitochondrial volume fraction $f_V = 0.18$ and the average mitochondrial dimensions: $0.6 \mu\text{m}$ diameter \times $2.4 \mu\text{m}$ long. For heart there is no obvious relation to the structure. The fact that the restriction is small may account for the difficulty in identifying the cause. It is possible that the characteristic dimension associated with the cell size ($15 \mu\text{m}$ diameter cylinder) in rat cardiac muscle (25) is just beginning to be observed at the longest times Δ used in these studies.

Limits on Restrictive Dimensions

As discussed under Evaluation of Restrictive Lengths, a dimension L may be determined when the diffusivity decreases as Δ is increased through the value $\Delta_R \simeq L^2/$

TABLE IV
CALCULATION OF EFFECTIVE VOLUME FRACTION
CONTRIBUTING TO RESTRICTED DIFFUSION

Type of sample studied	Observed diffusivity ratios		Effective volume fraction f_R	Observed restrictive length L
	Unrestricted D_S/D_w	Restricted D_R/D_w		
				μm
1 μm alumina				
Pure H_2O	1.00	0.75	0.167	5
26% Gly/ H_2O	0.50	0.40	0.133	4
47% Gly/ H_2O	0.25	0.18	0.187	4
Rat tissue				
Heart	0.37	0.34	0.08	10
Liver	0.30	0.25	0.17	2.7

$2D_S$, where D_S is the diffusivity for $\Delta \ll \Delta_R$. In order to prevent loss of signal greater than 90%, we must keep $\Delta_R < \Delta_{\text{max}} = 2.3 T_2 = 110$ ms for heart and 60 ms for liver. The upper limit for observable restrictive dimensions is then $L_{\text{max}} = (2D_S\Delta_{\text{max}})^{1/2} = 13.5 \mu\text{m}$ for heart and $8.5 \mu\text{m}$ for liver.

The lower limit $\Delta_{\text{min}} < \Delta_R$ is set by the need to avoid overlap by the tail of the first gradient pulse with the second τ_f pulse. For the equipment used in these experiments $\Delta_{\text{min}} = 2$ ms. This gives a minimum observable dimension $L_{\text{min}} = (2D_S\Delta_{\text{min}})^{1/2} = 1.5 \mu\text{m}$ for red blood cells.

SUMMARY

Results for PGSE-NMR measurements of restricted diffusion with characteristic lengths in the range from 1.5 to $15 \mu\text{m}$ in animal tissues and model inhomogeneous systems were summarized in Table II. The equipment and procedures for making these measurements were described, and the significance of the results were discussed.

For solution of macromolecules and particles much smaller than $0.5 \mu\text{m}$ the asymptotic diffusivity at long diffusion times was estimated from the Wang theory and compared with the results. For blood plasma, bound water about $\frac{1}{2}$ the volume of nonaqueous material was indicated. For cellular tissues slightly larger volumes of bound or trapped water would be required. In model systems containing particles of known average size and separation the observed characteristic dimension for restriction of diffusion by loosely packed particles was two to four times larger than either the particle size or the distance between individual particles.

For cells the size of a human red blood cell ($2\text{--}8 \mu\text{m}$), restriction by the cell membrane was indicated. A value for the permeability of the red cell membrane (0.014 cm/s) can be estimated from the change in diffusivity attributed to the restriction.

For cells as large as those found in heart and liver, restriction of diffusivity by intracellular structures typically shows only small changes. A volume fraction of intracellular space associated with the characteristic dimension of the restriction can be estimated from the magnitude of the change in diffusivity. The small change found in heart was not related to the structure in an obvious way. Comparison with the model systems indicates that particles about $0.7\ \mu\text{m}$ in diameter and occupying about 17% of the cell volume may be responsible for the restriction in liver, suggesting the mitochondria.

This research was supported in part by a National Science Foundation contract (NSF-C733), a grant from the Washington State Heart Association, and a Pulmonary Specialized Center of Research grant HL 14152 from the National Heart and Lung Institute.

Received for publication 4 June 1973 and in revised form 7 November 1973.

REFERENCES

1. COOPER, R. L., D. B. CHANG, A. C. YOUNG, C. J. MARTIN, and B. ANCKER-JOHNSON. 1973. *Bul. Am. Phys. Soc.* **18**: 410. (Abstr. EG6)
2. LING, G. N. 1969. *Int. Rev. Cytol.* **26**:1.
3. WANG, J. H. 1954. *J. Am. Chem. Soc.* **76**:4755.
4. WOESSNER, D. E. 1963. *J. Phys. Chem.* **67**:1365.
5. TANNER, J. E., and E. O. STEJSKAL. 1968. *J. Chem. Phys.* **49**:1768.
6. STEJSKAL, E. O., and J. E. TANNER. 1965. *J. Chem. Phys.* **42**:288.
7. STEJSKAL, E. O. 1965. *J. Chem. Phys.* **43**:3597.
8. PACKER, K. J., C. REES, and D. J. TOMLINSON. 1971. In *Diffusion Processes*. Vol. I. J. N. Sherwood et al., editors. Gordon & Breach, Inc., New York.
9. CARR, H. Y., and E. M. PURCELL. 1954. *Phys. Rev.* **94**:630.
10. ABETSEDARSKAYA, L. A., F. G. MIFTAKHUTDINOVA, and V. D. FEDOTOV. 1968. *Biofizika (Transl.)*. **13**:750.
11. HANSEN, J. R. 1971. *Biochim. Biophys. Acta*. **230**:482.
12. FINCH, E. D., J. F. HARMON, and B. H. MULLER. 1971. *Arch. Biochem. Biophys.* **147**: 299.
13. CHANG, D. C., C. F. HAZELWOOD, B. L. NICHOLS, and H. E. RORSCHARCH. 1972. *Nature (Lond.)*. **235**:170.
14. LOWE, I. J., and C. E. TARR. 1968. *J. Phys. E (J. Sci. Instrum.) Ser 2*. **1**:320, 604.
15. TANNER, J. E. 1965. *Rev. Sci. Instrum.* **36**:1086.
16. HODGMAN, C. D. et al., eds. *Handbook of Chemistry and Physics*. 1952. Chemical Rubber Publishing Co., Cleveland, Ohio. 34th edition. 1895.
17. BIRD, R. B., J. O. HIRSCHFELDER, and C. F. CURTISS. 1958. In *Handbook of Physics*. E. U. Condon and H. Odishaw, editors. McGraw-Hill, New York. 5-59.
18. CRICK, F. 1970. *Nature (Lond.)*. **225**:420.
19. ALTMAN, P. L., and D. S. DITMER. 1961. *Biological Handbooks: Blood and Other Body Fluids*. Federation of American Societies for Experimental Biology, Bethesda, Md.
20. ALTMAN, P. L., and D. S. DITMER. 1964. *Biological Handbooks: Biology Data Book*. Federation of American Societies for Experimental Biology, Bethesda, Md.
21. SHA'AFI, R. I., G. T. RICH, V. W. SIDEL, W. BOSSERT, and A. K. SOLOMON. 1967. *J. Gen. Physiol.* **50**:1377.
22. DICK, D. A. T. 1966. *Cell Water*. Butterworths, Washington, D.C.
23. DAVID, H. 1964. *Submikroskopische Ortho- und Patho-Morphologie der Leber*. Akademie-Verlag, Berlin.
24. WEIBEL, E. R., W. STÄUBLI, H. R. GNÄGI, and F. A. HESS. 1969. *J. Cell Biol.* **42**:68.
25. FABIATO, A., and F. FABIATO. 1972. *Circ. Res.* **31**:293.